1-1-2013

Rho/ROCK pathway is essential to the expansion, differentiation, and morphological rearrangements of human neural stem/progenitor cells induced by lysophosphatidic acid

Frisca Frisca
University of Melbourne

Duncan E. Crombie
Australia & Royal Victorian Eye and Ear Hospital, University of Melbourne

Mirella Dottori
University of Melbourne, mdottori@uow.edu.au

Yona Goldshmit
Australia & Royal Victorian Eye and Ear Hospital, Monash University

Alice Pebay
University of Melbourne, Australia & Royal Victorian Eye and Ear Hospital

Rho/ROCK pathway is essential to the expansion, differentiation, and morphological rearrangements of human neural stem/progenitor cells induced by lysophosphatidic acid

Abstract

We previously reported that lysophosphatidic acid (LPA) inhibits the neuronal differentiation of human embryonic stem cells (hESC). We extended these studies by analyzing LPA's effects on the expansion of neural stem/ progenitor cells (NS/PC) derived from hESCs and human induced pluripotent stem cells (iPSC), and we assessed whether data obtained on the neural differentiation of hESCs were relevant to iPSCs. We showed that hESCs and iPSCs exhibited comparable mRNA expression profiles of LPA receptors and producing enzymes upon neural differentiation. We demonstrated that LPA inhibited the expansion of NS/PCs of both origins, mainly by increased apoptosis in a Rho/Rho-associated kinase (ROCK)-dependent mechanism. Furthermore, LPA inhibited the neuronal differentiation of iPSCs. Lastly, LPA induced neurite retraction of NS/ PC-derived early neurons through Rho/ROCK, which was accompanied by myosin light chain (MLC) phosphorylation. Our data demonstrate the consistency of LPA effects across various sources of human NS/PCs, rendering hESCs and iPSCs valuable models for studying lysophospholipid signaling in human neural cells. Our data also highlight the importance of the Rho/ROCK pathway in human NS/ PCs. As LPA levels are increased in the central nervous system (CNS) following injury, LPA-mediated effects on NS/ PCs and early neurons could contribute to the poor neurogenesis observed in the CNS following injury.

Disciplines

Medicine and Health Sciences

Publication Details

Frisca, F., Crombie, D. E., Dottori, M., Goldshmit, Y. & Pebay, A. (2013). Rho/ROCK pathway is essential to the expansion, differentiation, and morphological rearrangements of human neural stem/progenitor cells induced by lysophosphatidic acid. Journal of Lipid Research, 54 (5), 1192-1206.

Rho/ROCK pathway is essential to the expansion, differentiation, and morphological rearrangements of human neural stem/progenitor cells induced by lysophosphatidic acid[S]

Frisca Frisca,* Duncan E. Crombie,*,† Mirella Dottori,§ Yona Goldshmit,†, and Alice Pébay[1,*,†]**

Department of Ophthalmology,* University of Melbourne, East Melbourne VIC, Australia; Centre for Eye Research,† Australia & Royal Victorian Eye and Ear Hospital, East Melbourne VIC, Australia; Department of Anatomy and Neurosciences,§ University of Melbourne, Parkville VIC, Australia; and Australian Regenerative Medicine Institute,** Monash University, Clayton, VIC, Australia

Abstract **We previously reported that lysophosphatidic acid (LPA) inhibits the neuronal differentiation of human embryonic stem cells (hESC). We extended these studies by analyzing LPA's effects on the expansion of neural stem/progenitor cells (NS/PC) derived from hESCs and human induced pluripotent stem cells (iPSC), and we assessed whether data obtained on the neural differentiation of hESCs were relevant to iPSCs. We showed that hESCs and iPSCs exhibited comparable mRNA expression profiles of LPA receptors and producing enzymes upon neural differentiation. We demonstrated that LPA inhibited the expansion of NS/PCs of both origins, mainly by increased apoptosis in a Rho/Rho-associated kinase (ROCK)-dependent mechanism. Furthermore, LPA inhibited the neuronal differentiation of iPSCs. Lastly, LPA induced neurite retraction of NS/PC-derived early neurons through Rho/ROCK, which was accompanied by myosin light chain (MLC) phosphorylation. Our data demonstrate the consistency of LPA effects across various sources of human NS/PCs, rendering hESCs and iPSCs valuable models for studying lysophospholipid signaling in human neural cells. Our data also highlight the importance of the Rho/ROCK pathway in human NS/PCs. As LPA levels are increased in the central nervous system (CNS) following injury, LPA-mediated effects on NS/PCs and early neurons could contribute to the poor neurogenesis observed in the CNS following injury.**—Frisca, F., D. E. Crombie, M. Dottori, Y. Goldshmit, and A. Pébay. **Rho/ROCK pathway is essential to the expansion, differentiation, and morphological rearrangements of human neural stem/progenitor cells induced by lysophosphatidic acid.** ***J. Lipid Res.*** **2013.** 54: **1192–1206.**

Supplementary key words human embryonic stem cell • induced pluripotent stem cell • Rho pathway

Lysophosphatidic acid (LPA) is a bioactive lysophospholipid that induces pleiotropic effects in many cell types. LPA mainly acts through binding to its specific G-protein-coupled receptors LPA_{1-5}, which can couple to G_i, G_q, G_{12}, and possibly G_s, to modulate specific downstream signaling pathways (1). LPA can also activate the purinergic receptors LPA_6/P2Y5 (2), GPR87 (3), and P2Y10 (4), the transient receptor potential vanilloid receptor 1 cation channel (TRPV1) (5), and the intracellular peroxisome proliferator-activator receptor (PPAR) γ (6). LPA receptors are expressed in various types of stem cells and demonstrate a differential expression profile across various cells and tissues (7, 8). LPA can be synthesized both intracellularly and extracellularly by activation of different enzymes (1); however, it is not yet entirely clear whether or how intracellular LPA contributes to extracellular signaling. Although LPA can be synthesized extracellularly by secreted phospholipases A, in particular by the secreted PLA_2 group IIA ($sPLA_2$), a major source of extracellular LPA in the central nervous system (CNS) most probably arises from the activity of the secreted lysophospholipase D enzyme autotaxin (ATX), as this enzyme

This work was supported by a National Health and Medical Research Council of Australia Career Development Award Fellowship (A.P.), a Transport Accident Commission project grant (A.P.), and the Victorian State Government's Department of Innovation, Industry and Regional Development's Operational Infrastructure Support Program. F.F. received an Australian Development Scholarship (ADS) by the Australian government (AusAID).

Manuscript received 15 September 2012 and in revised form 1 March 2013.

Published, JLR Papers in Press, March 4, 2013
DOI 10.1194/jlr.M032284

Abbreviations: ATX, autotaxin; bFGF, basic fibroblast growth factor; CNS, central nervous system; EFG, epidermal growth factor; hESC, human embryonic stem cell; hPSC, human pluripotent stem cell; iPSC, induced pluripotent stem cell; LPA, lysophosphatidic acid; MLC, myosin light chain; NBM, neural basal media; NEP, neuroepithelium cell line; NS/PC, neural stem/progenitor cell; ROCK, Rho-associated kinase; TUNEL, terminal transferase dUTP nick end labeling.

[1]To whom correspondence should be addressed.
e-mail: apebay@unimelb.edu.au

[S] The online version of this article (available at http://www.jlr.org) contains supplementary data in the form of one video.

is found to be expressed in various CNS regions during development or adulthood, and its activity is modified following various physiopathological events (1). In the CNS, LPA can target most cell types and plays roles in a variety of developmental and pathological processes, including neurogenesis, neuropathic pain, neural injury, schizophrenia, epilepsy, and memory impairment (1).

Neural stem/progenitor cells (NS/PC) have been extensively studied, with the aim of using endogenous and/or donor NS/PCs to replace neurons and restore circuitry in a neurodegenerative microenvironment. In theory, human embryonic stem cells (hESC) and human induced pluripotent stem cells (iPSC) are a great source of cells to generate NS/PCs and progeny, which could potentially be used for transplantation and also to provide insight into human neurogenesis. Although not identical, hESCs and iPSCs seem very similar, but the extent of the variations and similarities between the two types of cells remains open (9). Hence, comparing their differentiation potentials and response to specific signaling molecules is still required to allow drawing conclusions on whether hESCs and iPSCs show critical differences. It was previously shown in hESCs that the bone morphogenetic protein inhibitor noggin induces neuroectodermal differentiation, as shown by the expression of SOX2, paired box protein 6, and nestin and a lack of expression of early mesoderm or endoderm markers (10). Once dissected, these colonies are propagated in suspension in neural basal media (NBM) supplemented with basic fibroblast growth factor (bFGF) and epidermal growth factor (EGF), where they aggregate and form a spherical-like cluster named neurosphere, which consists of a heterogeneous population of NS/PCs (10). Neurospheres can be differentiated to give rise to neurons and glia when plated onto laminin or fibronectin substrates, respectively. Hence, this differentiation protocol allows the progressive neural patterning of human pluripotent stem cells (hPSC, noggin stage), efficient generation and expansion of NS/PCs (neurosphere stage), and subsequent differentiation into early neurons and glial cells (11). Other protocols of differentiation have been established for hESCs (12), including protocols that maintain NS/PCs as a monolayer instead of a neurosphere, but they are less defined. This overall method allows to precisely divide the whole differentiation process into defined stages and to efficiently generate human neural progenitors and early neurons, rendering this technique robust and well defined. These features make this protocol highly useful for the study of fundamental signaling mechanisms involved in NS/PC multipotency and expansion. Unraveling these mechanisms may allow for better and more efficient techniques to use human NS/PCs, either endogenous or exogenous, to treat neurodegeneration and inflammation of the CNS by characterizing, for instance, how the cellular environment modifies NS/PC fate in term of survival and differentiation.

LPA's effects on NS/PCs and neuroblasts seem to vary depending on the origin of the cells (8). These differences might be the consequence of discrepancies in terms of cell source (different lines and differentiation stages), heterogeneity of cell populations, species, LPA receptor expression profiles, LPA concentration used, and the culture conditions of the cell lines. In rodents, LPA was reported to stimulate, inhibit, or not affect NS/PC proliferation (13–16). Further, LPA has been shown to be a survival factor, a pro-apoptotic agent or a prodifferentiation factor of NS/PCs (16–18). Comparably, LPA has also been described as a proliferative, survival, or prodifferentiation factor in some neuroblasts but not all (8). It was recently shown that LPA can induce fetal hydrocephalus in the mouse by an aberrant activation of Lpa_1 on NS/PCs during development (19). LPA also acts through the Rho pathway to induce morphological rearrangements in neuroblasts and neurons (20–24), including actin polymerization (21) that leads to the formation of retraction fibers, neurite retraction (21, 25–32), cell rounding (26, 29, 33, 34), cluster compaction (35–38), and growth cone collapse (21, 26, 27).

The study of LPA in human NS/PCs and neurons is still extremely limited. Although we briefly reported that LPA inhibits the ability of hESC-derived NS/PCs to form neurospheres, we did not attempt to characterize this biological effect and the signaling pathways associated (39). We also previously showed that when two-week-old hESC-derived neurospheres were plated onto laminin or fibronectin, LPA inhibited their neuronal differentiation through the Rho/ROCK and phosphatidylinositol 3-kinase (PI3K)/Akt pathways (39). This effect was linked to an antidifferentiation effect of LPA, as no modification in apoptosis or proliferation could be detected on these plated neurospheres (39). Hurst and colleagues, however, reported that LPA stimulates proliferation and cell-rounding of hESC-derived neuroepithelium cell line (NEP), a stable line enriched in hESC-derived NS/PCs and grown under adherent conditions (40, 41). These variations may be due to culture conditions or cell origin.

Here and given the potential differences of hESCs and human iPSCs, we dissected LPA's effects on the progressive neural differentiation on both types of hPSCs, thus allowing to directly compare LPA signaling in hESCs and human iPSCs. Our differentiation protocol allows to assess effects of LPA on NS/PCs during their neural differentiation and on NS/PC-derived neurons. While our previous study concentrated on the impact of LPA on the neuronal and glial differentiation of hESC-derived NS/PCs (39), this current study assessed the effects of LPA at an earlier stage of neuralization, namely, the expansion of NS/PCs, from both hESCs and human iPSCs. Further, we assessed whether the data obtained on the neuronal and glial differentiation of hESCs were relevant to human iPSCs, allowing us to draw conclusions on the similarity of LPA's effects across these two different cell types. Finally, we assessed LPA's effects on the morphology of early human neurons derived from NS/PCs. This study thus provides a comprehensive assessment of the role of LPA in these various differentiation stages on hESCs and human iPSCs. Because LPA is released upon inflammation and is involved in neurotrauma and various CNS diseases (1), appreciating its role on neurogenesis and

understanding its impact, specifically on NS/PCs and progeny, is relevant to transplantation work. LPA might be the environmental cue that is able to modify the behavior of NS/PCs and their derivatives during inflammation after neurotrauma.

MATERIALS AND METHODS

Ethics

All experiments were approved by the Human Research Ethics Committees of the University of Melbourne (Approvals 0605017 and 0830010).

Reagents

Dilutions of LPA (Sigma-Aldrich, Castle Hill, Australia) were made in 0.1% fatty acid-free BSA (final concentration 0.01% BSA; Sigma-Aldrich). Cells were treated with LPA (up to 10 μM), LPA_1/LPA_3 antagonists Ki16425 (Sigma-Aldrich, 10 μM), LY294002 (Promega, 10 μM), Y27632 (Biomol, 1 μM), GW9662 (Cayman Chemicals, 1 μM), cell-permeable C3 Transferase (Cytoskeleton, 1 ng/ml, pretreament 4 h), *Pertussis* toxin (PTX, Biomol, 10 ng/ml, pretreament 18 h). Unless otherwise specified, inhibitors were added to cells 30 min prior to addition of LPA to the culture medium on the first incubation.

RT-PCR

mRNA was isolated from undifferentiated hPSCs, noggin-treated hPSCs, NS/PCs in neurospheres, and monolayers of NS/PCs using Dynabeads Oligo (dT)25 (Dynabeads). RT-PCR were conducted using High Capacity cDNA Reverse Transcriptase Kit (Applied Biosystems), following the manufacturer's instructions. A negative control (−RT) consisting in the absence of reverse transcriptase was performed to check the absence of genomic DNA. qPCR was carried out using TaqMan Universal master mix (Applied Biosystems) and the 7900HT Fast Real-Time PCR system (Applied Biosystems) and TaqMan gene expression assays for LPA_{1-5} and *ATX* (Applied Biosystems). TaqMan gene expression assays for LPA_1 (Hs00173500_m1), LPA_2 (Hs00173704_m1), LPA_3 (Hs00173857_m1), LPA_4 (Hs00271072_s1), LPA_5 (Hs01051307_m1), *ATX* (Hs00196470_m1), *PLA2-group IIA* (Hs00179898_m1), *ROCK1* (Hs01127699_m1), and *ROCK2* (Hs00178154_m1) were used (Applied Biosystems). The relative quantitation was achieved by applying the comparative CT method (ΔΔCT) in which the mRNA levels were normalized against the level of glyceraldehyde-3-phosphate dehydrogenase (GAPDH) mRNA (TaqMan gene expression assay Hs99999905_m1) or β-actin (Hs99999903_m1) with LPA_5 used as the reference. Q-PCR reaction of the non-reverse-transcribed sample was also conducted for each Taqman probe above to check the genomic DNA contamination in the sample and the specificity of the probes.

Immunofluorescence

Following fixation with paraformaldehyde (PFA) 4% for 10 min, cells were blocked in a 10% fetal calf serum-PBS 0.1% Tween 20 (PBT, 60 min) and immunostained with the following primary antibodies: mouse anti-βIII-tubulin (Millipore); rabbit anti-glutamate aspartate transporter (GLAST, Millipore); rabbit anti-glial fibrillary acidic protein (GFAP, DAKO); mouse anti-A2B5 (Millipore); rabbit anti-nestin (Millipore); rabbit anti-doublecortin (DCX, Abcam); mouse phospho-myosin light chain (MLC) 2 (Ser19); and rabbit phospho-cofilin (Ser3) (77G2, Genesearch). Cells were then immunostained with the appropriate conjugated secondary antibodies (Alexa Fluor 555 or 488, Cy3, Molecular Probes-Invitrogen). Nuclei were counterstained with 4′,6-diamidino-2-pheylindole (DAPI, 1:1000, Sigma-Aldrich). Specificity of the staining was verified by the appropriate negative control immunoglobulin fraction (see Fig. 4G, H, Fig. 5F, G). For monolayer NS/PCs, cells were permeabilized with PBS-Tween/0.3% Triton X-100 following PFA fixation.

Cell culture and neural induction of hPSCs

The iPS (Foreskin) 4 clone 1 and clone 2, abbreviated iPS1 and iPS2 (42), and the hESC line ENVY (ES Cell International) were cultured as described (43, 44). Neuronal induction by noggin (R and D, 500 ng/ml) was performed as described in (11). Noggin-treated cells were dissected after 14 days and were further subcultured in suspension in NBM together with bFGF (Millipore) and EGF (R and D, 20 ng/ml each) to form neurospheres (45).

NS/PC monolayer culture

The monolayer culture of NS/PCs was generated as previously reported (46) with some modifications. Briefly, two-week-old neurospheres cultured with NBM supplemented with bFGF and EGF were collected and dissociated by disaggregation with Trysin-EDTA (Invitrogen). The enzymatic reaction was stopped using soybean trypsin inhibitor (Sigma). The dissociated cells were seeded in NBM supplemented with growth factors onto precoated tissue culture dishes with laminin 1 μg/cm^2 (Sigma-Aldrich) to generate a monolayer of NS/PCs. The medium was changed every second day. NS/PCs were further passaged with accutase (Sigma). Medium was changed every second day, and cells were cultured for three weeks. All experiments were consistently conducted on less than passage 5 monolayered NS/PCs.

Neurosphere formation assay

Noggin-treated cells were harvested after 14 days by dissecting and further subcultured as neurospheres, in suspension in NBM together with bFGF and EGF (20 ng/ml each), in the presence or in the absence of LPA (complete with any inhibitor used), with medium changed every second day (39). Each condition was performed in at least eight individual wells and repeated in at least three independent experiments. Assessment of neurosphere formation was performed after 7 days.

Neuronal and glial differentiation of neurosphere

After two weeks in suspension, neurospheres cultivated in NBM with bFGF and EGF were plated as previously described (11) onto poly-l-lysine/laminin-coated (Sigma, 10 and 5 μg/ml, respectively) or poly-l-lysine/fibronectin-coated (Millipore, 10 μg/ml) dishes in NBM lacking growth factors to induce neuronal and glial differentiation, respectively, allowed to attach, and incubated in the presence or in the absence of LPA (complete with any inhibitor used) for five days (39). For each type of experiment, after attachment, medium was changed every second day. Pictures were taken of each individual well (inverted microscope Olympus IX71 and Cell IR software) following five days in culture. The cells were then fixed with 4% PFA/PBS.

Quantification of neuron-forming spheres

Quantification was performed by counting the number of spheres from which neuronal outgrowth was observable (39). In some cases neurospheres failed to attach, independently of the treatments, and these floating neurospheres were excluded from quantification.

Cell morphology assays

Six- to seven-day-old neurospheres cultured on poly-l-lysine/laminin-coated slides were placed on the heated stage of an inverted microscope (Olympus) equipped with phase-contrast optics and temperature control. During time-lapse recording, the plated neurospheres were maintained in 25 mM HEPES-buffered NBM (pH 7.4) at 37°C and observed continuously using a camera connected to Axiovision time-lapse software (Carl Zeiss). Various concentrations of LPA and/or selected inhibitors were applied during time-lapse recording. To observe reversibility of LPA's effect, LPA was withdrawn from the culture medium and replaced by normal 25 mM HEPES-buffered complete medium, followed by time-lapse recording at indicated times. Images were acquired using 5 s interframe intervals. The pictures were then assessed for morphological modifications of plated neurosphere and neurite retraction. At least three independent experiments were performed for each treatment.

Apoptosis and proliferation assays

Cell apoptosis was quantified by measuring numbers of condensed nuclei with terminal transferase dUTP nick end labeling (TUNEL) immunocytochemistry. TUNEL analysis was performed using the In Situ Cell Death Detection Kit (Roche) following the manufacturer's instruction. Proliferation was assessed by staining with Ki67 (Thermo Fisher Scientific, Clone SP6). Briefly, day 7 neurospheres were collected, manually dissociated, centrifuged onto glass slides (4 min at 1,000 rpm, Shandon Cytospin 4, Thermo Fisher Scientific), air dried, fixed with 4% PFA, and permeabilized with 0.1% Triton X-100 before immunostaining with a TMR Red-conjugated TdT enzyme or Ki67, respectively. Apoptosis and proliferation were also assessed on laminin-plated, two-week-old neurospheres treated with or without LPA (10 μM, 18 h) as described in Ref. 39. Cell nuclei were counterstained with DAPI. Specificity of the staining was verified by the absence of staining in negative controls without the TdT enzyme or negative isotype. Apoptosis and proliferation were respectively quantified by manually counting TUNEL-positive cells and Ki67-positive cells as a percentage of total cell number, counting at least 1,000 cells per treatment by using Image J software (National Institutes of Health).

RhoA activation assay

Active RhoA was measured using the G-LISA RhoA activation assay biochem kit (Cytoskeleton, colorimetric assay) according to the manufacturer's instructions. Briefly, monolayered NS/PCs were cultured for two days in NBM supplemented with bFGF and EGF (20 ng/ml) until they reached 30–50% confluency. Concentration of bFGF and EGF was reduced to 10 ng/ml for one day and then removed overnight prior to treatment. Cells were treated or not with LPA 10 μM for 1, 3, 5, 15, and 30 min. Following treatments, cells were rinsed twice with cold PBS, rapidly scraped, lysed in a cold premixed lysis buffer with protease inhibitor on ice, and centrifuged (1,000 *g*, 4°C, 1 min). Supernatants were collected and snap-frozen in liquid nitrogen. Some aliquots were taken for protein concentration measurement. Following adjustment of protein concentration, G-LISA was then processed according to manufacturer's kit instruction. The optical density (OD) was read at 490 nm using a 96-well microplate reader (Bio-Rad).

NS/PC monolayer differentiation

To induce neuronal and astrocytic differentiation, the monolayer NS/PCs were replated onto poly-l-ornithine/laminin-treated wells at 1–5 × 10^4 cells/cm^2. Medium was changed every second day, and cells were cultured for three weeks.

LPA treatment in the maintenance of monolayer NS/PC culture

NS/PCs were seeded onto laminin-precoated 24-well plates in NBM supplemented with growth factor (bFGF and EGF, 20 ng/ml each). After two days, medium was changed and supplemented with LPA and fixed in PFA 4% 18 h later.

Cell morphology assays of the differentiated neurons derived from monolayer NS/PC culture

Neurons cultured for three weeks on poly-l-lysine/laminin-coated slides were placed on the heated stage of an inverted microscope (Olympus) equipped with phase-contrast optics and temperature control. During time-lapse recording, the plated neurons were maintained in 25 mM HEPES-buffered NBM (pH 7.4) at 37°C and observed continuously using a camera connected to time-lapse software (Axiovision and Olympus IX71). LPA at different concentrations (0.1, 1, and 10 μM) was applied during time-lapse recording. Images were acquired using 5 s interframe intervals.

siRNA knockdown of ROCK

Monolayer NS/PCs were passaged into complete NBM media without antibiotic one day before transfection at 2.5–5 × 10^5/well in 6-well plates. Knockdown of ROCKI and/or ROCKII was performed using Dharmacon SMART pool ON-TARGETplus ROCK1 siRNA (L-003536-00-0005) and ON-TARGETplus ROCK2 siRNA (L-004610-00-0005), which were already demonstrated to be specific in hESC (47). Control for transfection was done using ON-TARGETplus NonTargeting Pool (D-001810-10-05). Specific siRNA (25 nM) for each pool was mixed with Dharmafect II, following Dharmacon siRNA Transfection's protocol. Measurement of knockdown efficiency and survival were respectively performed at 48 h and 72–96 h following transfection. Quantification of *ROCKI* and *ROCKII* mRNA levels were determined by qPCR. Expression levels of corresponding genes were normalized to the housekeeping gene β-actin and expressed as the percentage level over the control. At 48 h post transfection, cells were passaged onto laminin-coated chamber slides. At 72 h post transfection, LPA (10 μM) was added for 18 h prior to TUNEL assay.

Statistical analysis

All sets of experiments were performed at least three times in triplicate, unless specified (*n* refers to the number of independent experiments performed on different cell cultures). Datasets were expressed as means ± SEM. Significance of the differences was evaluated using the *t*-test or the one- and two-way ANOVA followed by the Newman-Keuls test for multiple comparisons. Statistical significance was established at $*P < 0.05$, $**P < 0.01$, and $***P < 0.001$.

RESULTS

Neural differentiated hPSCs express $LPA_{1–5}$ and LPA producing enzymes mRNA

We performed qPCR analysis of hPSCs at the different stages of progressive neural differentiation (undifferentiated cells, noggin-treated cells, and neurospheres) to characterize their expression profile (**Fig. 1**). All of the undifferentiated and the differentiated hPSCs expressed $LPA_{1–5}$, *ATX*, and $sPLA_2$ mRNA (Fig. 1), with LPA_2 and

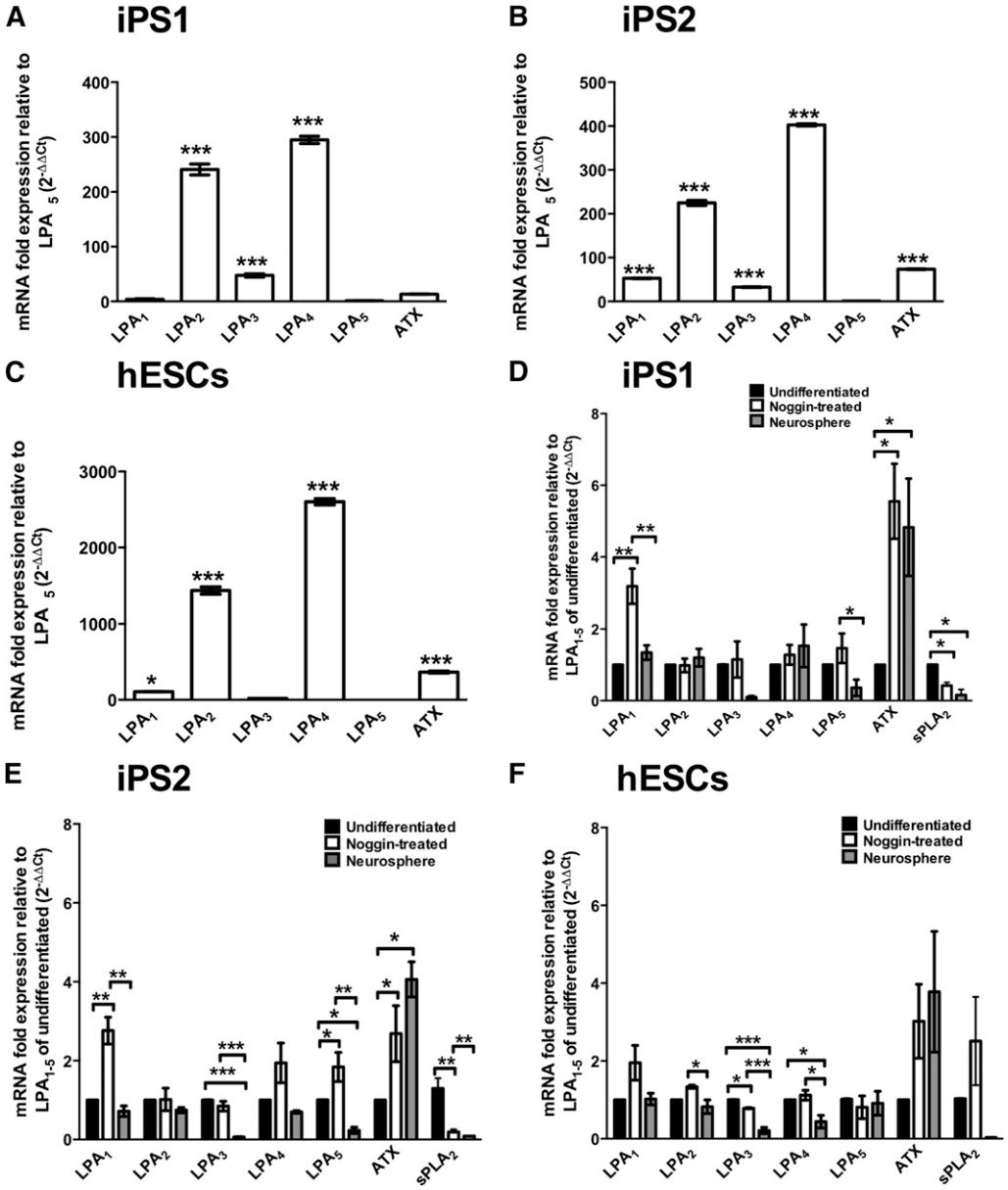

Fig. 1. *$LPA_{1–5}$, ATX, and $sPLA_2$* gene expression profile in neural differentiated hPSCs. (A–C) mRNA expression ($2^{-\Delta\Delta Ct}$) profile of *$LPA_{1–5}$, ATX* in neurosphere relative to LPA_5 in iPS1 (A), iPS2 (B), and hESCs (C). (D–F) mRNA profile of undifferentiated and progressively differentiated into NS/PCs (noggin-treated and neurosphere) relative to undifferentiated iPS1 (D), iPS2 (E), and hESCs (F). The mRNA expression levels were normalized against the level of *GAPDH* mRNA (ΔCt) with the level of *LPA_5* (A–C) or *$LPA_{1–5}$, ATX*, and *$sPLA_2$* of the undifferentiated hPSCs (D–F) used as the reference genes (ΔΔCt). Data were obtained from at least three independent experiments and expressed as means ± SEM of triplicates of each sample. The statistical analysis was established by one-way ANOVA; $*P < 0.05$; $**P < 0.01$; $***P < 0.001$.

LPA_4 mRNA being the most abundant. LPA_5 mRNA was expressed at very low levels in neurospheres obtained from all lines relative to *$LPA_{1–4}$* (Fig. 1A–C). To examine the expression profile of LPA receptors, ATX, and *$sPLA_2$* at each differentiation stage, the mRNA expression levels of each gene were presented in comparison to their corresponding levels in undifferentiated hPSCs (Fig. 1D–F). Fig. 1D provides an illustration of the data obtained with iPS1. Temporal upregulation of *LPA_1* mRNA expression was found during early differentiation (noggin-treated stage), followed by a downregulation during later differentiation (neurosphere stage). Similarly, an increase of *ATX* mRNA expression was observed in both noggin-treated cells and neurospheres. *LPA_3* and *LPA_5* mRNA were downregulated upon neural differentiation, and no significant modulation was observed for *LPA_2* and *LPA_4*. Very low levels of *$sPLA_2$* were observed at all stages of differentiation. Similar trends were observed in the other lines tested (Fig. 1E, F). Given the similar trend of expression of *$LPA_{1–5}$, ATX*, and *$sPLA_2$* mRNA in neurospheres from the two clones of iPSCs, we assessed most biological effects of LPA in iPS1 and compared them with hESCs.

LPA inhibits neurosphere formation through activation of the Rho/ROCK pathway

We previously reported that one dose of LPA (10 μM) significantly inhibits neurosphere formation of hESC-derived NS/PCs, without further description of this effect (39). Here, we observed a similar effect in two clones of iPSCs and characterized this in both iPSCs and hESCs (**Figs. 2** and **3**). Interestingly, LPA-mediated inhibition of neurosphere formation is dose dependent in iPS1 and hESCs and shows a similar trend in iPS2, although not statistically significant (Figs. 2C and 3A, F). As exemplified in Fig. 2A–C in iPS1, LPA strongly inhibited sphere formation in a dose-dependent manner (LPA, 10 μM: 10.4 ± 3.8% of sphere formation compared with control: 59.4 ± 7.5%, n > 3, $P < 0.001$; Fig. 2A–C). This effect was associated with a decrease in proliferation (36.11 ± 10.1% of

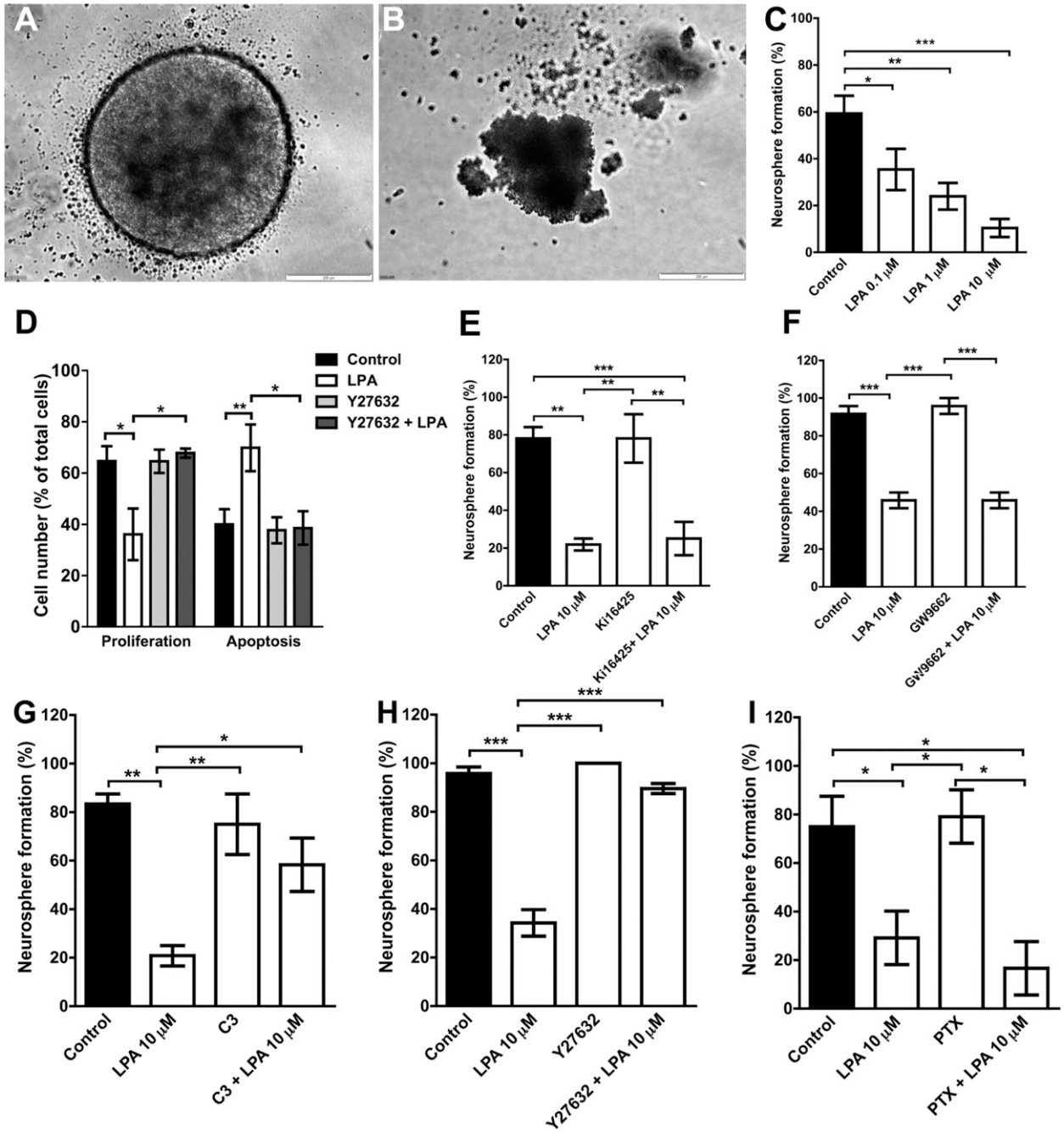

Fig. 2. LPA inhibits neurosphere formation of hPSC-derived NS/PCs. Representative images of neurosphere in the absence (**A**) or presence of LPA (10 μM, B) for seven days. (C) Quantification of neurosphere formation in the absence (Control) or presence LPA at various concentrations. (D) Quantification of proliferation (Ki67) and apoptosis (TUNEL) in neurospheres treated or not (Control) with LPA (10 μM) and/or Y27632 (1 μM) for seven days. (E–I) Quantification of neurosphere formation in the absence (Control) or presence of LPA (10 μM) and/or Ki16425 (10 μM, E), GW9662 (1 μM, F), C3 (1 ng/ml, G), Y27632 (1 μM, H), and PTX (10 ng/ml, I). The specific inhibitors were preincubated as specified in Materials and Methods prior to LPA addition and maintained in the culture medium for the entire differentiation period. Data are expressed as mean ± SEM from at least three independent experiments. The statistical analysis was established by one-way ANOVA analysis (C–I); $*P < 0.05$; $**P < 0.01$; $***P < 0.001$. Data presented were obtained with iPS1. Scale bar: 200 μm.

Ki67-positive cells in LPA-treated cells versus 64.67 ± 5.84% in control conditions, n > 3, $P < 0.01$; Fig. 2D) as well as an increase in apoptosis (LPA: 69.86 ± 9.1% of cells were TUNEL-positive versus 40.03 ± 5.9% in control, n > 3, $P < 0.01$; Fig. 2D). A similar trend was observed in hESCs, although the decreased proliferation was not found to be statistically significant (Fig. 3J).

Quantifying neurosphere formation frequency does not discriminate between apoptosis and proliferation but provides a reliable and robust measurement of NS/PC expansion and was used here to identify the signaling mechanisms used by LPA during this process. The impact of LPA on neurosphere formation was found not to be mainly through its extracellular receptors $LPA_{1/3}$, as pretreatment with Ki16425 at a dose that is specifically antagonistic to $LPA_{1/3}$ (48) did not modify LPA-mediated inhibition of sphere formation in the iPSCs but significantly reduced the effect of LPA on hESC sphere formation (Figs. 2E and 3B, G). It is likely that the blockage of these receptors is compensated by the other LPA receptors present in NS/PCs. Due to the lack of commercially available, specific LPA receptor antagonists, the involvement of the other receptors was not assessed in this study. Further, we decided not to use siRNA in these experiments because of the poor transfection efficiency due to the three-dimensional structure of the sphere. Instead, siRNA knockdown of *ROCKI/II* were performed on monolayered NS/PCs as explained below. In the presence of the selective PPARγ antagonist GW9662 (49), the effect of LPA was not modified, suggesting that LPA does not act through PPARγ to inhibit neurosphere formation (Fig. 2F).

In all cell lines, the effect of LPA on sphere formation was abolished by pretreatment with either the specific Rho inhibitor C3 exoenzyme (50) (Figs. 2G and 3C, H) or with the p160 ROCK inhibitor Y27632 used at a dose specific to p160ROCK inhibition (51) (Figs. 2H and 3D, F), which alone have no marked effect, indicating that LPA acts through the Rho/ROCK pathway to inhibit neurosphere formation. Furthermore, when cells were incubated with PTX, which ADP-ribosylates α_i proteins, LPA's effect was maintained (Figs. 2I and 3E, I), suggesting that LPA's effect is not $G_{i/o}$ mediated and is consistent with a $G_{12/13}$ Rho-mediated mechanism. This data was confirmed by measuring apoptosis and proliferation of NS/PCs in the presence of LPA and Y27632 (Figs. 2D and 3J). The sole application of Y27632 did not modify basal proliferation or apoptosis (Figs. 2D and 3J). As shown in Fig. 2 in iPS1, LPA-induced apoptosis and LPA-reduced proliferation were abolished by Y27632 (Fig. 2D). Thus, this data indicate that LPA acts through the Rho/ROCK pathway to inhibit neurosphere formation, at least by increasing cell apoptosis and by decreasing proliferation in iPS1.

LPA induces RhoA activation

To confirm that LPA modulated NS/PC expansion by activation of the Rho/ROCK pathway, we measured Rho activity in NS/PCs by using an adherent culture of human NS/PCs derived from dissociated neurospheres. This protocol was favored over spheres, as the monolayer NS/PC culture ensures an even exposure of LPA to all cells at the same time, which cannot be controlled in three-dimensional neurospheres. The adherent monolayered culture expressed the NS/PC marker nestin (**Fig. 4A**, B), could be subcultured for several passages, reformed neurospheres in suspension culture (Fig. 4C), could be differentiated into neurons and glial cells (Fig. 4D–F) and also express mRNA for LPA receptors and producing enzymes (Fig. 4I). Similar trends in LPA-mediated effects were observed between suspension culture and adherent culture of NS/PCs, thus allowing parallel conclusions to be made between the two culture systems (Fig. 4J–M). Adherent NS/PCs were cultured in the presence or absence of LPA, followed by Rho activation measurements by ELISA. A basal level of Rho activation was detected on control NS/PCs. As shown in Fig. 4N, LPA induced a rapid increase of active RhoA (GTP-Rho) in NS/PCs, which was biphasic with an elevation that peaked at 1 min post exposure followed by a sustained but lower activity for at least 30 min. This result directly demonstrates that LPA stimulates Rho in NS/PCs and that this activation critically modulates NS/PC expansion.

To exclude potential off-targets of the ROCK kinase inhibitor Y27632 despite its high specificity, we further confirmed our results by a molecular approach consisting of knocking down *ROCKI* and *ROCKII* by siRNA in monolayered NS/PCs, individually or together (Fig. 4O, P). Following 48 h post transfection, single siRNA treatment for either *ROCKI* or *ROCKII* specifically knocked down its corresponding gene while their dual knocking down resulted in 75.6 ± 7.0% and 76.2 ± 4.3% downregulation of *ROCKI* and *ROCKII* mRNAs (Fig. 4O). When monolayered NS/PCs were knocked down for both ROCKI/ROCKII, the apoptosis induced by LPA was abolished, demonstrating the involvement of ROCK in LPA's effect (Fig. 4P).

LPA inhibits the neuronal differentiation of iPSCs through the Rho/ROCK and PI3K/Akt pathways

LPA did not modify glial differentiation of iPSC-derived neurospheres but inhibited their neuronal differentiation (**Fig. 5A–**G). This effect was dose dependent and ROCK and PI3K/Akt dependent (Fig. 5H, I). As shown in Fig. 5I, LPA's effect on human iPSC-derived NS/PCs was partially abolished by the sole application of Y27632 or LY294002 but was abolished in the presence of both inhibitors. These effects were observed in both iPSC lines tested. As previously observed with hESC-derived neurospheres (39), we confirm here that LPA acts through an inhibition of differentiation rather than by modifying proliferation or apoptosis of these two-week-old neurospheres. Indeed, neurospheres plated onto laminin in the presence of LPA (10 μM, 18 h) did not show modification of Ki67 or TUNEL when compared with control conditions (no LPA; Fig. 5J).

LPA induces morphological rearrangements of hPSC-derived early neurons through the Rho/ROCK pathway

After six days of plating, neurospheres had already given rise to βIII-tubulin-positive early neurons, which radially migrate out from the edges of the neurospheres (**Fig. 6**). When incubated with LPA, these early neurons underwent rapid neurite retraction, leading to cell rounding (occurs

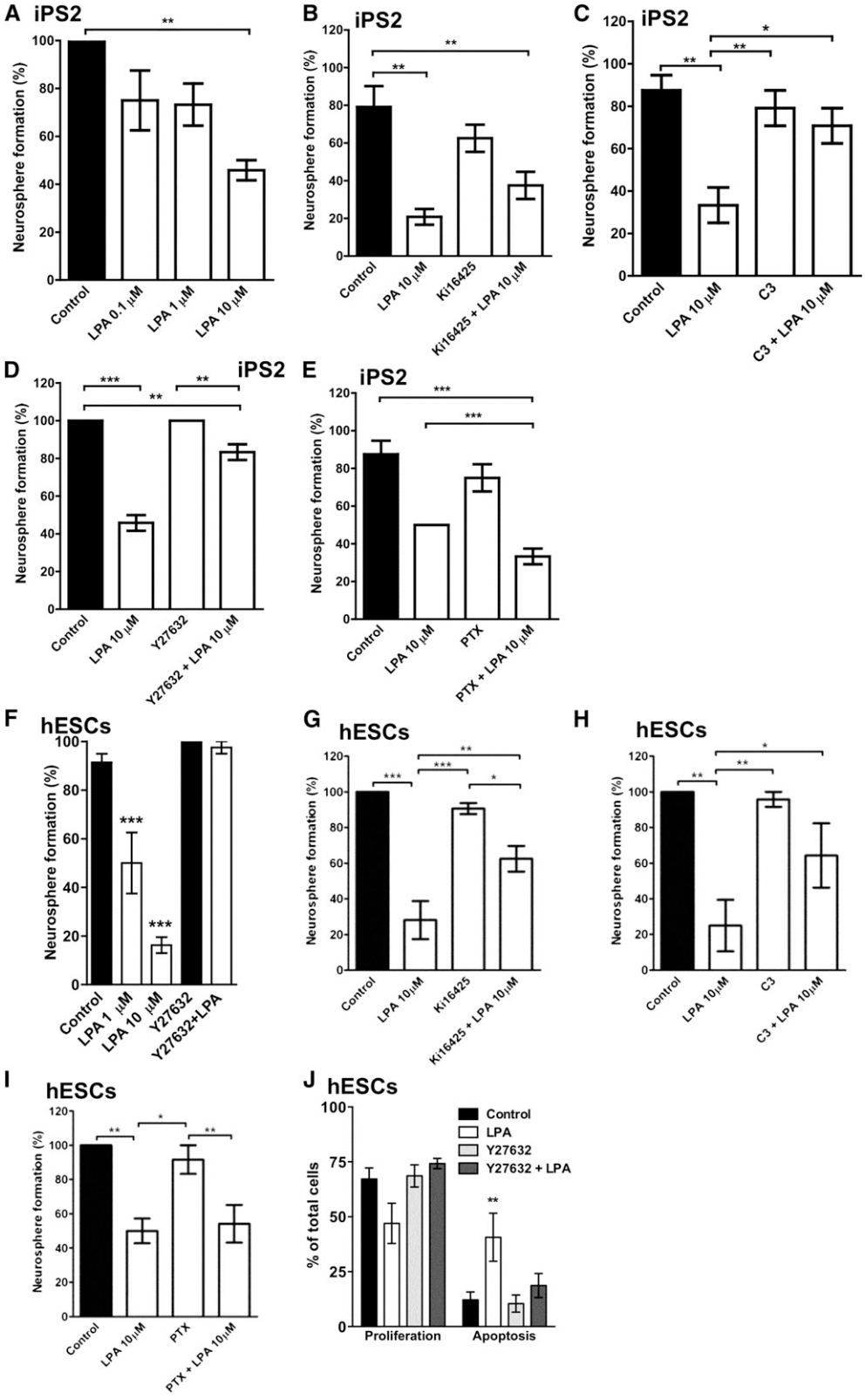

Fig. 3. LPA inhibits neurosphere formation of iPS2- and hESC-derived NS/PCs. Quantification of neurosphere formation in the absence (Control) or presence of LPA at various concentration in iPS2 (A–E) and hESCs (F–I), with or without Ki16425 (10 μM, B, G), C3 (1 ng/ml, C, H), Y27632 (1 μM, D, F), and PTX (10 ng/ml, E, I). (J) Quantification of proliferation (Ki67) and apoptosis (TUNEL) in hESC neurospheres treated or not (Control) with LPA (10 μM) and/or Y27632 (1 μM) for seven days. The specific inhibitors were preincubated as specified in Materials and Methods prior to LPA addition and maintained in the culture medium for the entire differentiation period. Each panel represents a pool of at least three independent experiments, and data are expressed as means ± SEM. The statistical analysis was established by one-way ANOVA analysis; $*P < 0.05$; $**P < 0.01$; $***P < 0.001$.

within minutes; Fig. 6A–D and supplementary video I). These effects were dose dependent, starting at 1 μM, and reversible (**Table 1** and Fig. 6E–G). The reversibility took longer when compared with the rapid retraction observed in the presence of LPA, but it suggest that the neurite retraction was not the result of cell death.

LPA-induced morphological rearrangements could be prevented by preincubation with C3 exoenzyme or Y27632 (Table 1, Fig. 6H–K, and supplementary video I), indicating that LPA acts through the Rho/ROCK pathway to induce neurite retraction in early neurons derived from hPSCs. PTX and LY294002 had no effect on LPA-induced neurite retraction (Table 1), indicating that this mechanism is $G\alpha_i$ and PI3K/Akt independent. Similar data were observed in early neurons derived from monolayered NS/PC cultures (Fig. 4K, L). To further elucidate LPA's role in neural development, we analyzed the impact of LPA on the actin-myosin cytoskeleton, assessing cofilin and MLC, respectively, as these proteins are downstream effectors of ROCK (52). These experiments were performed on monolayered NS/PCs by immunohistochemistry to assess localization of phospho-cofilin and phospho-MLC. As shown in Fig. 6L–O, although we did not observe an effect of LPA on phospho-cofilin, LPA induced the phosphorylation of MLC, suggesting that it induces morphological rearrangements through modification of myosin.

DISCUSSION

LPA is bioactive lipid known to affect most cell types of the nervous system. Limited studies have addressed LPA's role in the human CNS and in human neural cells. We previously described that LPA inhibits the neuronal differentiation of hESC-derived NS/PCs and briefly reported that LPA inhibits neurosphere formation of hESCs (39). Here we established a comprehensive in vitro system to assess the role of LPA at multiple stages of human neural differentiation using both hESCs and human iPSCs. We assessed whether these two different sources of human NS/PCs are equivalent in terms of LPA's effects upon neuralization by describing $LPA_{1–5}$, *ATX*, and $sPLA_2$ mRNA expression and by assessing whether effects previously observed with hESCs were retrieved in human iPSCs. We also characterized how LPA modifies NS/PC expansion and the morphology of early human neurons. We observed a similar pattern of effects of LPA throughout the neural differentiation of hESCs and iPSCs. The three lines tested expressed LPA receptors and *ATX* and $sPLA_2$ mRNA with a similar profile. In all NS/PCs tested, LPA increased cell death and inhibited neuronal differentiation without modifying glial differentiation. Furthermore, LPA induced morphological rearrangements in early neurons differentiated from NS/PCs. In iPSC-derived NS/PCs, LPA also significantly decreased proliferation, while a similar trend was observed in hESC-derived NS/PCs but without reaching statistical significance. Hence, our data shows generally consistent results across different iPSC and hESC lines, with some minor interline differences in responsiveness to LPA, indicating that the mechanisms mediated by LPA are fundamental in neural differentiation and are not influenced by other variables often observed between different hESC/iPSC lines (53).

Our results show that both undifferentiated hPSCs and neural differentiated hPSCs express $LPA_{1–5}$ mRNA, confirming our previous RT-PCR data (8, 39, 54), and they show that LPA_2 and LPA_4 are the most abundant mRNA in undifferentiated hPSCs and neurospheres. Modulation in the receptor expression profile was observed following neural differentiation with an upregulation of LPA_1 mRNA during the early neural commitment of hPSCs (noggin-treated stage), followed by its downregulation during later differentiation (neurosphere stage). The mRNA expression profile in hPSC-derived neurospheres shared some similar trends to the profile observed in hESC-derived NEP (41) and in the monolayer NS/PCs, with $LPA_{1,2,4}$ being the most expressed mRNA. The low level of $sPLA_2$ expression and the presence of *ATX* mRNA following neural differentiation, as exemplified in this data, are consistent with the fact that *ATX* expression is associated with neurogenesis (55).

As LPA_1 shows its highest expression level at the noggin stage, we assessed its involvement in neurosphere formation as readout of the impact of LPA on NS/PC expansion. Using the $LPA_{1–3}$ antagonist Ki16425, we observed no significant effect of this treatment on LPA's effect in iPSCs and a partial inhibition in hESCs, suggestive that other receptors are involved in the inhibition of NS/PC expansion by LPA. This is consistent with the fact that $LPA_{2,4}$ are the most abundant mRNAs in NS/PCs from all cell lines. LPA receptors are coupled to multiple G proteins, with $LPA_{1–5}$ coupled to G_q, $LPA_{1,2,4,5}$ coupled to G_{12}, $LPA_{1–4}$ coupled to G_i, and $LPA_{4,5}$ also coupled to G_s (1). PTX did not affect LPA's effect on sphere formation, suggesting that LPA acts independently of α_i, either through G_{12} and/or G_q and/or the $\beta\gamma$ subunits of G proteins. This is highly likely given that the main receptors present at either the noggin stage or neurosphere stage ($LPA_{2,\,4\,>\,1}$) signal through G_q and G_{12}. Additionally, as LPA's effect on NS/PC expansion is Rho/ROCK-mediated, it is also probable that the mechanism is G_{12} dependant (56). Further, we showed that LPA inhibits neuronal differentiation of iPSC-derived NS/PCs through the PI3K/Akt and Rho/ROCK pathways, which are likely to be mediated by $\beta\gamma$ and G_{12}, respectively (56), and which is consistent with our previous data obtained with hESCs (39). Lastly, we describe that LPA induces morphological rearrangements of early neurons in a Rho/ROCK manner, presumably mediated by G_{12}. Altogether, this data demonstrates the importance of LPA receptor-mediated signaling along the whole neural differentiation process.

We found that LPA promoted apoptosis of early human NS/PCs, as revealed by neurosphere formation assay, which is consistent with some NS/PC and neuroblast studies performed in rodents (16, 17, 38, 57, 58) but differs with others in which LPA improves cell survival (16, 38) or proliferation (13, 35, 59). In human cells, we previously showed that LPA does not modify apoptosis of older hESC-derived NS/PCs (39) as, when two-week-old hESC-derived

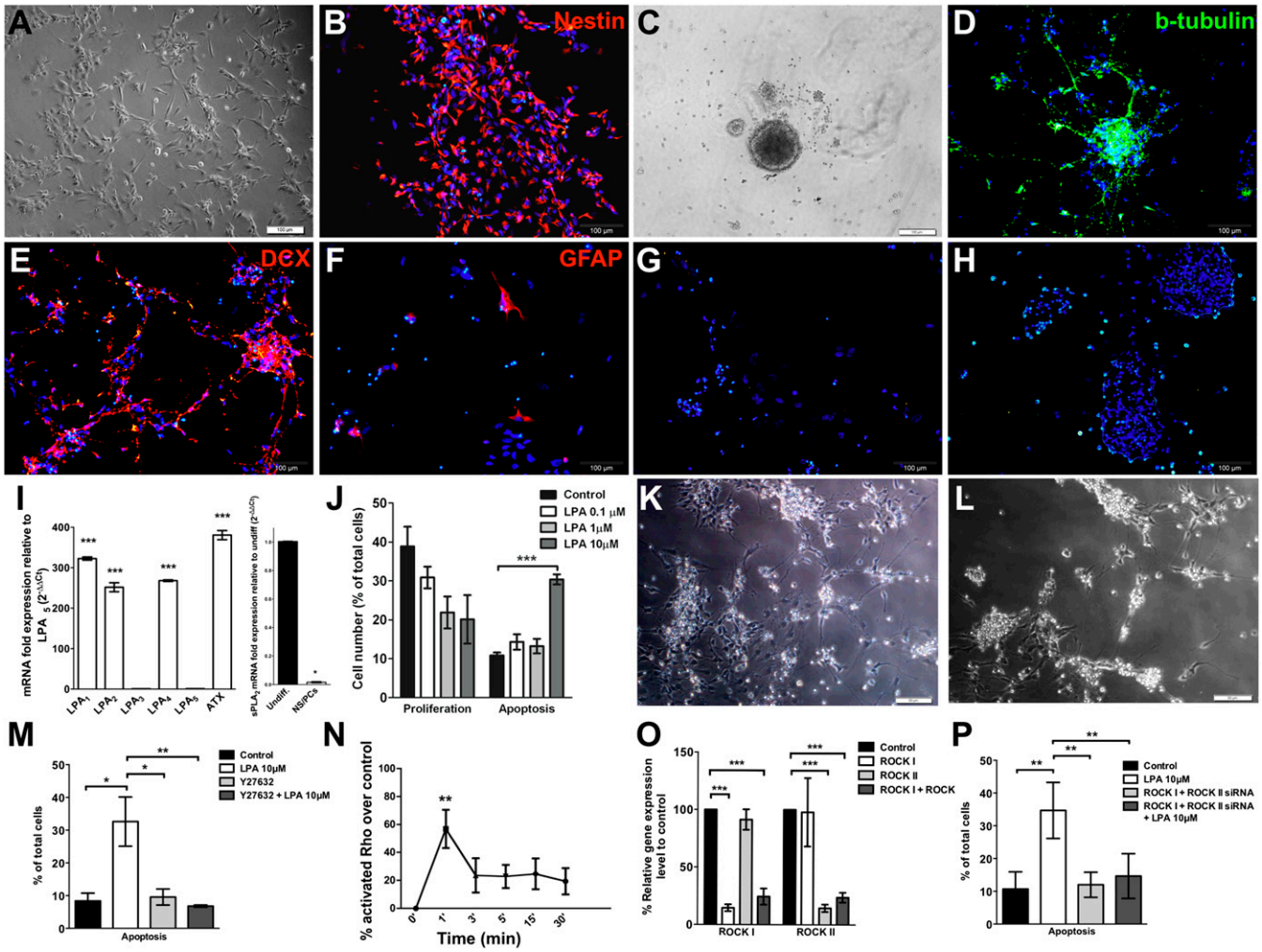

Fig. 4. Characteristics of adherent NS/PC in culture. (A–F) Representative images of plated NS/PCs showing brightfield (A) and immunostaining for nestin (red) and DAPI (blue, B). (C) Representative brightfield image of a neurosphere formed from plated NS/PCs. (D–F) Representative immunostaining of NS/PCs differentiated into neurons with βIII-tubulin (green, D), DCX (red, E), and glial cells with GFAP (red, F) and DAPI counterstain (blue). (G) Rabbit and (H) mouse negative isotype controls. (I) mRNA expression ($2^{-\Delta\Delta Ct}$) profile of LPA_{1-5}, *ATX*, and $sPLA_2$ in NS/PCs. For LPA_{1-5} and *ATX* mRNA, expression levels were normalized against the level of GAPDH mRNA (ΔCt) with the level of LPA_5 used as the reference gene (ΔΔCt); $sPLA_2$ was expressed compared with undifferentiated cells to show its very low level of expression. (J) Quantification of proliferation (Ki67) and apoptosis (TUNEL) in plated NS/PCs treated or not (Control) with various doses of LPA (0.1–10 µM) for 18 h. (K, L) Representative images of early neurons from monolayered NS/PCs cells prior to treatment (K) and treated with LPA (10 µM) for 20 min (L) showing morphological rearrangements. (A–H, K, L) Data are representative pictures of at least three independent experiments. Scale bars are indicated within each image. (M) Quantification of apoptosis (TUNEL) in plated NS/PCs treated or not (Control) with LPA (10 µM) and/or Y27632 (1 µM) for 18 h. (N) Time course of activated RhoA (GTP Rho) by LPA measured at 490 nm by ELISA in monolayered NS/PCs. (O) mRNA expression profile of *ROCKI* and *ROCKII* following knockdown of *ROCKI* and/or *ROCKII* by siRNA for 48 h. mRNA expression levels were normalized against the level of β-actin mRNA and are expressed as percentage of control. (P) Quantification of apoptosis (TUNEL) in siRNA control pool (Control, LPA) or ROCK I- and ROCK II-treated monolayer NS/PCs subsequently incubated in the absence or presence of LPA (10 µM) for 18 h. (I, J, M–P) Data were obtained from at least three independent experiments and are expressed as means ± SEM of triplicates of each sample. The statistical analysis was established by one-way ANOVA; $*P < 0.05$; $**P < 0.01$; $***P < 0.001$.

neurospheres plated in conditions allowing differentiation were incubated with LPA for 18 h, no modification in apoptosis or proliferation was detected by TUNEL or BrdU assays, respectively (39). Here we confirmed this data using human iPSC-derived neurospheres. Further, others demonstrated that LPA increases growth of hESC-derived NEP (41), an effect observed at a concentration of up to 0.1 µM. In this study, that concentration already inhibited sphere formation but did not significantly affect monolayered NS/PCs. Similarly, LPA inhibits neuronal differentiation but not glial differentiation of human iPSCs, which is in agreement with our previous study using hESCs (39) and with data obtained in rodents (58); although other studies found opposite effects in various NS/PCs and neuroblasts (14, 17, 18, 38, 59, 60).

Even though using similar protocols of maintenance of NS/PCs as monolayers, it is interesting to note that we observe some variations with data obtained on hESC-derived NEP (41). In particular, as shown in Fig. 4, we did not observe the growth effect of low doses of LPA on monolayers of NS/PCs described by others (41), but we showed

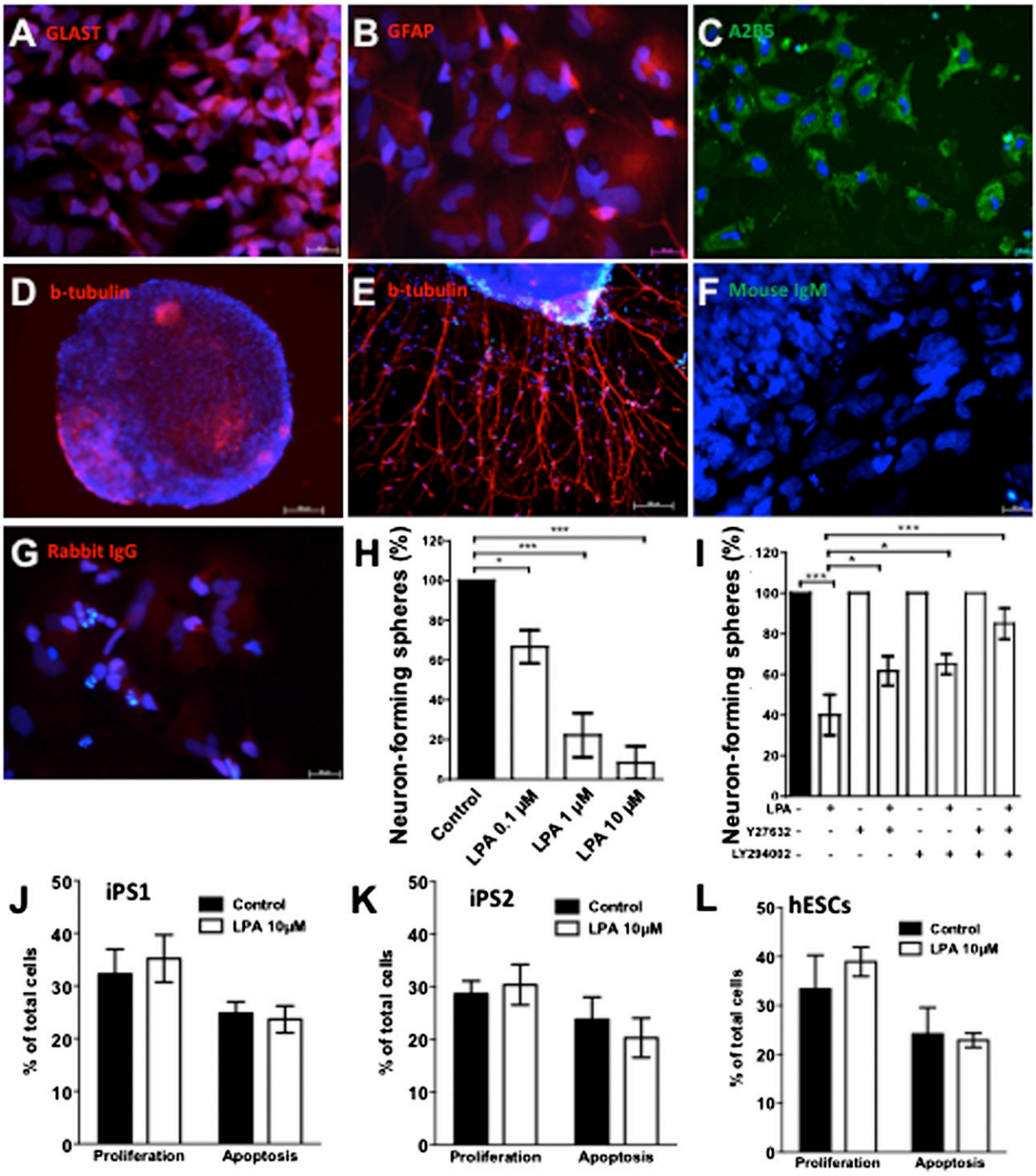

Fig. 5. LPA inhibits neuronal differentiation of human iPSCs without modifying apoptosis and proliferation. (A–C) Immunostaining of glial differentiation of neurospheres plated onto fibronectin and incubated in the presence of LPA (five days, 10 µM) with GLAST (A), GFAP (B), or A2B5 (C) antibodies with DAPI counterstain (blue). (D, E) βIII-tubulin immunostaining (red) and DAPI counterstain (blue) of neurospheres plated onto laminin and incubated in the presence of LPA (five days, 10 µM, D) or in its absence (E). (F) Mouse and (G) rabbit negative isotype controls. Data are representative pictures of at least three independent experiments. Scale bars: A–C, F–G: 20 µm; D, E: 100 µm. (H, I) The percentage of neuron-forming neurospheres was quantified in the presence of various concentrations of LPA (H) or in the absence (Control) or presence of LPA (10 µM) and/or Y27632 (1 µM) and/or LY 294002 (10 µM) (I). (J–L) Proliferation and apoptosis by Ki67 and TUNEL quantification, respectively, of two-week-old neurospheres plated onto laminin in the absence (Control) or in the presence of LPA (10 µM) for 18 h in iPS1 (J), iPS2 (K), and hESCs (L). (H–L) Data are expressed as means ± SEM of at least three independent experiments. The statistical analysis was established by one-way ANOVA analysis (H, I) or *t*-test (J–L); $*P < 0.05$; $**P < 0.01$; $***P < 0.001$. (A–J) Data presented were obtained with iPS1.

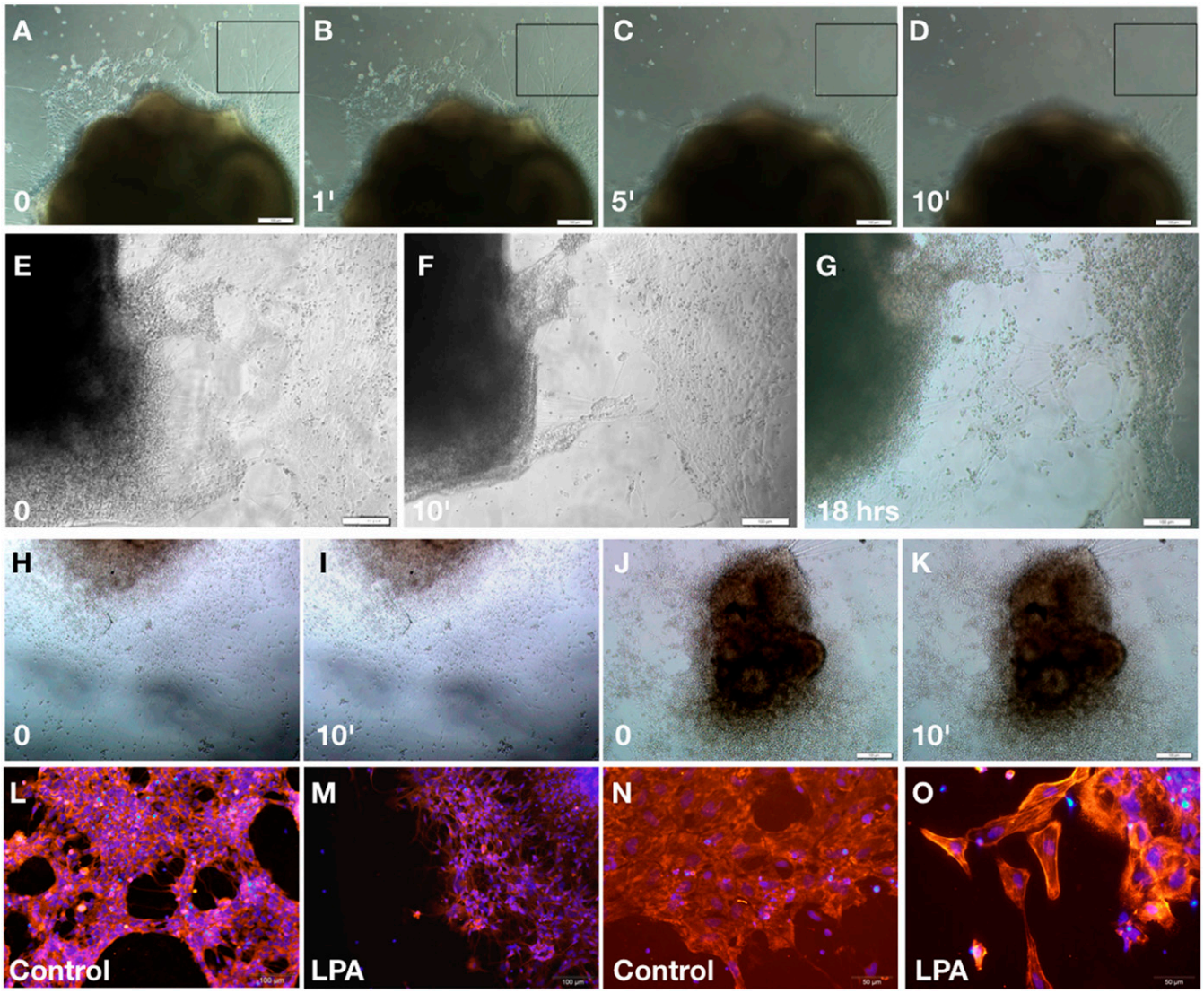

Fig. 6. LPA induces morphological rearrangements in early neurons derived from hPSCs. Representative images of cells prior to treatment (0, A, E) and treated with LPA (10 μM) for 1, 5, and 10 min (1′, 5′, 10′, C–D); or treated with LPA (10 μM) for 10 min (F) and then incubated with normal medium for 18 hrs (G); or preincubated with C3 (1 ng/ml, H) or Y27632 (1 μM, J), prior to addition of LPA (10 μM, I, K) for 10 min. Data presented were obtained with iPS1. Square shows example of an area showing retractions. Scale bar: 100 μm. (L–O) Representative immunostained images of early neurons in control or following LPA treatment (10 μM, 15 min) with phospho-cofilin (L, M) or phospho-MLC antibody (N, O) and DAPI counterstain (blue).

that LPA induces apoptosis of the monolayer NS/PCs at a dose that was not previously tested in hESC NEP. Our data, using two different sources of human NS/PCs and two different protocols for maintenance (neurospheres and monolayers), indicates that the observed pro-apoptotic effects of LPA are consistent, regardless of the NS/PC origin. It is thus likely that the variations between our data and those of Hurst and colleagues in terms of cell growth at low concentrations of LPA are due to a difference in the populations of human cells studied. In particular, the main difference between the protocols for generating a monolayer of NS/PCs is in the derivation of the NS/PCs themselves. We use dissociated neurospheres to obtain a monolayered culture, whereas the NEP used by Hurst and colleagues were directly obtained from hESCs without going through a neurosphere stage (41, 46). This variation in protocol might account for the discrepancies in LPA-mediated effects between the studies, which could reflect a variation in the developmental state (either more or less restricted) of the human NS/PC populations in use.

LPA has been extensively studied for its prominent effect in inducing cytoskeletal rearrangements. In particular, LPA is shown to induce neurite retraction and cell rounding through the Rho/ROCK pathway in rodent immortalized neuroblasts and PC12 (26, 61). We observed a similar pattern of morphological changes in early human neurons, which, following exposure to LPA, underwent immediate and rapid retraction, cell rounding, and migration to form cell clusters and compaction in a Rho/ROCK-dependent manner. Interestingly, in hESC NEP, LPA induced ROCK-dependent morphological rearrangements, but these were observed to be slow, peaking around 5 h (41).

JOURNAL OF LIPID RESEARCH ASBMB

TABLE 1. Neurite retraction in early neurons derived from hPSCs

Tested Agents	Neurite Retraction (+/−)
Control	−
LPA 0.1 μM	−
LPA 1 μM	+
LPA 10 μM	+
Y27632 1 μM	−
Y27632 + LPA 10 μM	−
C3	−
C3 +LPA 10 μM	−
PTX	−
PTX + LPA 10 μM	+
LY294002	−
LY294002 + LPA 10 μM	+

LPA's effect in neurite retraction among tested agents in human NS/PCs. Early neurons differentiated from hPSCs were incubated or not with LPA and/or Y27632 (1 μM, 30 min preincubation), C3 transferase (1 ng/ml, 4 h preincubation), PTX (10 ng/ml, 18 h preincubation), and LY 294002 (10 μM, 30 min preincubation). +, retraction; −, no retraction. Each treatment assessment is representative of at least three independent experiments.

The importance of the Rho/ROCK pathway in stem cell survival is now established. The ROCK inhibitor Y27632 significantly increases hESC single-cell survival (62, 63) and NS/PCs following neurosphere dissociation (64). Further, upon dissociation to single cells, the Rho/ROCK pathway is activated and responsible for modulating cell-cell contact-induced apoptosis in hESCs (65), NS/PCs (64), and neurons (66), an effect associated with MLC phosphorylation in hESCs (47). Moreover, in neurons, Rho/ROCK activation induces apoptotic membrane blebbing by stimulating MLC phosphorylation (66) and has associations to neuronal death following spinal cord injury (67). Other data suggest that ROCK inhibition may not act directly by reducing apoptosis but rather by desensitizing cells to their environment and thus limiting apoptosis (68).

Our data showing LPA's activation of RhoA is in line with data obtained by others in other stem and progenitor cells (1) and are the first demonstration of human-derived NS/PCs at various stages of differentiation. A large body of evidence shows that LPA acts through the Rho pathway to modify cell survival, apoptosis, and proliferation in diverse types of cells by mediating cell shape/focal adhesion alteration (38, 69, 70). Our current data demonstrate that LPA activates RhoA in human NS/PCs and implicate this pathway in LPA-induced apoptosis, decreased proliferation, and together with the PI3K/Akt pathway, LPA inhibition of neuronal differentiation of human NS/PCs. Furthermore, activation of this pathway is essential to LPA-induced morphological rearrangements in human NS/PC-derived early neurons.

Adult NS/PCs are present in the CNS, predominantly in neurogenic regions, such as the subventricular zone and hippocampus. They have been reported to migrate to sites of injury and tumors (71), effects likely to be linked to the repair of damaged tissue. Furthermore, evidence suggests that NS/PCs contribute to neurogenesis in the adult mouse and human following stroke (72, 73). Similar data were observed following brain injury in the juvenile rat (74). Following CNS injury, ischemia, or events that damage the blood brain barrier, LPA-like activity increased within the cerebrospinal fluid, levels of LPA within the CNS increased up to 10 μM (75–78), and levels of ATX increased within astrocytes neighboring a lesion of the adult rat brain (79). Our data using human cells suggest that the presence of LPA in regions of neurogenesis within the CNS may modify NS/PC survival and differentiation. Our data also suggest that high levels of LPA have the ability to be pro-apoptotic on human NS/PCs, to bias their differentiation toward glial cells and to induce neurite retraction and cell rounding of early neurons and thus limit the regenerative responses to injury. This is relevant to endogenous neurogenesis and might explain low levels of neurogenesis observed following trauma, with LPA being a limiting factor of genesis. This finding is also relevant to transplantation of human stem or progenitor cells within the CNS, as the inflammation present or generated by the transplantation procedure itself may induce increased levels of LPA which could limit neurogenesis and repair. Our data also suggest that neurogenesis may be enhanced by blockers of LPA signaling, such as LPA antibodies that we recently demonstrated were able to abolish LPA's effect on human NS/PCs in vitro and improve neuronal survival and functional recovery following spinal cord injury in vivo (80). Such a mechanism has already been proved with sphingosine-1-phosphate, as blocking its signaling enhances endogenous NS/PC migration to the injury site following trauma (81).

CONCLUSION

LPA plays a broad role in human NS/PCs and their neural derivatives, regulating expansion, differentiation, and morphology. We showed that in hPSC-derived NS/PCs, LPA increases apoptosis, decreases proliferation, inhibits neuronal differentiation, and induces rapid morphological rearrangements in early neurons. All these effects are at least Rho/ROCK dependent. We observed that the effects of LPA on NS/PCs are insensitive to PTX treatment, indicating no involvement of α_i but suggestive of the involvement of α_{12}, α_q, or β/γ in these biological effects. LPA-induced activation of Rho/ROCK is likely to be G_{12} mediated, as this is the common upstream G protein for Rho and has been reported to be involved in the pro-apoptotic effect of LPA through $LPA_{1,2,4}$ (16). Thus, our data demonstrate the consistency in the effect of LPA across various sources of human NS/PCs, rendering hESCs and human iPSCs valuable in vitro models for studying lysophospholipid signaling in human neural cells. Our data also highlight the importance of the Rho/ROCK pathway in human NS/PC expansion and differentiation. It is thus possible that blocking LPA signaling in vivo, in which levels increase following trauma, would enhance neurogenesis.

The authors thank Guizhi Sun and Daniella Herszfeld (Monash University) for their help in setting up monolayer cultures of

NS/PCs; Dr. Hitesh Peshavariya and Dr. Guei-Sheung Liu (Centre for Eye Research Australia) for their advice with siRNA work; and Prof. James A. Thomson (University of Wisconsin) for providing the iPS(Foreskin) cell lines.

REFERENCES

1. Frisca F., R. A. Sabbadini, Y. Goldshmit, and A. Pébay. 2012. Biological effects of lysophosphatidic acid in the nervous system. *Int. Rev. Cell Mol. Biol.* **296:** 273–322.
2. Pasternack, S. M., I. von Kugelgen, K. A. Aboud, Y. A. Lee, F. Ruschendorf, K. Voss, A. M. Hillmer, G. J. Molderings, T. Franz, A. Ramirez, et al. 2008. G protein-coupled receptor P2Y5 and its ligand LPA are involved in maintenance of human hair growth. *Nat. Genet.* **40:** 329–334.
3. Tabata, K., K. Baba, A. Shiraishi, M. Ito, and N. Fujita. 2007. The orphan GPCR GPR87 was deorphanized and shown to be a lysophosphatidic acid receptor. *Biochem. Biophys. Res. Commun.* **363:** 861–866.
4. Murakami, M., A. Shiraishi, K. Tabata, and N. Fujita. 2008. Identification of the orphan GPCR, P2Y(10) receptor as the sphingosine-1-phosphate and lysophosphatidic acid receptor. *Biochem. Biophys. Res. Commun.* **371:** 707–712.
5. Nieto-Posadas, A., G. Picazo-Juarez, I. Llorente, A. Jara-Oseguera, S. Morales-Lazaro, D. Escalante-Alcalde, L. D. Islas, and T. Rosenbaum. 2012. Lysophosphatidic acid directly activates TRPV1 through a C-terminal binding site. *Nat. Chem. Biol.* **8:** 78–85.
6. McIntyre, T. M., A. V. Pontsler, A. R. Silva, A. St Hilaire, Y. Xu, J. C. Hinshaw, G. A. Zimmerman, K. Hama, J. Aoki, H. Arai, et al. 2003. Identification of an intracellular receptor for lysophosphatidic acid (LPA): LPA is a transcellular PPARgamma agonist. *Proc. Natl. Acad. Sci. USA.* **100:** 131–136.
7. Pébay, A., C. S. Bonder, and S. M. Pitson. 2007. Stem cell regulation by lysophospholipids. *Prostaglandins Other Lipid Mediat.* **84:** 83–97.
8. Pitson, S. M., and A. Pebay. 2009. Regulation of stem cell pluripotency and neural differentiation by lysophospholipids. *Neurosignals.* **17:** 242–254.
9. Yamanaka, S. 2012. Induced pluripotent stem cells: past, present, and future. *Cell Stem Cell.* **10:** 678–684.
10. Pera, M. F., J. Andrade, S. Houssami, B. Reubinoff, A. Trounson, E. G. Stanley, D. W. Ootswaard, and C. Mummery. 2004. Regulation of human embryonic stem cell differentiation by BMP-2 and its antagonist noggin. *J. Cell Sci.* **117:** 1269–1280.
11. Dottori, M., A. Pebay, and M. F. Pera. 2010. Neural differentiation of human embryonic stem cells. *In* Neural Stem Cells: Methods and Protocols. 2nd edition. L. P. Weiner, editor. Humana Press. 19–30.
12. Denham, M., and M. Dottori. 2009. Signals involved in neural differentiation of human embryonic stem cells. *Neurosignals.* **17:** 234–241.
13. Cui, H. L., and J. T. Qiao. 2006. Promotive action of lysophosphatidic acid on proliferation of rat embryonic neural stem cells and their differentiation to cholinergic neurons in vitro. *Sheng Li Xue Bao.* **58:** 547–555.
14. Svetlov, S. I., T. N. Ignatova, K. K. Wang, R. L. Hayes, D. English, and V. G. Kukekov. 2004. Lysophosphatidic acid induces clonal generation of mouse neurospheres via proliferation of Sca-1- and AC133-positive neural progenitors. *Stem Cells Dev.* **13:** 685–693.
15. Harada, J., M. Foley, M. A. Moskowitz, and C. Waeber. 2004. Sphingosine-1-phosphate induces proliferation and morphological changes of neural progenitor cells. *J. Neurochem.* **88:** 1026–1039.
16. Sun, Y., J-S. Nam, D-H. Han, N-H. Kim, H-K. Choi, J. K. Lee, H. J. Rhee, and S-O. Huh. 2010. Lysophosphatidic acid induces upregulation of Mcl-1 and protects apoptosis in a PTX-dependent manner in H19–7 cells. *Cell. Signal.* **22:** 484–494.
17. Fukushima, N., S. Shano, R. Moriyama, and J. Chun. 2007. Lysophosphatidic acid stimulates neuronal differentiation of cortical neuroblasts through the LPA1-G(i/o) pathway. *Neurochem. Int.* **50:** 302–307.
18. Rhee, H. J., J-S. Nam, Y. Sun, M-J. Kim, H-K. Choi, D-H. Han, N-H. Kim, and S-O. Huh. 2006. Lysophosphatidic acid stimulates cAMP accumulation and cAMP response element-binding protein phosphorylation in immortalized hippocampal progenitor cells. *Neuroreport.* **17:** 523–526.
19. Yung, Y. C., T. Mutoh, M-E. Lin, K. Noguchi, R. R. Rivera, J. W. Choi, M. A. Kingsbury, and J. Chun. 2011. Lysophosphatidic acid signaling may initiate fetal hydrocephalus. *Sci. Transl. Med.* **3:** 99ra87.
20. Saito, S. 1997. Effects of lysophosphatidic acid on primary cultured chick neurons. *Neurosci. Lett.* **229:** 73–76.
21. Fukushima, N., I. Ishii, Y. Habara, C. B. Allen, and J. Chun. 2002. Dual regulation of actin rearrangement through lysophosphatidic acid receptor in neuroblast cell lines: actin depolymerization by Ca(2+)-alpha-actinin and polymerization by rho. *Mol. Biol. Cell.* **13:** 2692–2705.
22. Fukushima, N., J. A. Weiner, D. Kaushal, J. J. A. Contos, S. K. Rehen, M. A. Kingsbury, K. Y. Kim, and J. Chun. 2002. Lysophosphatidic acid influences the morphology and motility of young, postmitotic cortical neurons. *Mol. Cell. Neurosci.* **20:** 271–282.
23. Sayas, C. L., A. Ariaens, B. Ponsioen, and W. H. Moolenaar. 2006. GSK-3 is activated by the tyrosine kinase Pyk2 during LPA1-mediated neurite retraction. *Mol. Biol. Cell.* **17:** 1834–1844.
24. Sayas, C. L., M. T. Moreno-Flores, J. Avila, and F. Wandosell. 1999. The neurite retraction induced by lysophosphatidic acid increases Alzheimer's disease-like Tau phosphorylation. *J. Biol. Chem.* **274:** 37046–37052.
25. Pai, K. S., and D. D. Cunningham. 2002. Geldanamycin specifically modulates thrombin-mediated morphological changes in mouse neuroblasts. *J. Neurochem.* **80:** 715–718.
26. Jalink, K., E. J. van Corven, T. Hengeveld, N. Morii, S. Narumiya, and W. H. Moolenaar. 1994. Inhibition of lysophosphatidate- and thrombin-induced neurite retraction and neuronal cell rounding by ADP ribosylation of the small GTP-binding protein Rho. *J. Cell Biol.* **126:** 801–810.
27. Kozma, R., S. Sarner, S. Ahmed, and L. Lim. 1997. Rho family GTPases and neuronal growth cone remodelling: relationship between increased complexity induced by Cdc42Hs, Rac1, and acetylcholine and collapse induced by RhoA and lysophosphatidic acid. *Mol. Cell. Biol.* **17:** 1201–1211.
28. Fukushima, N., Y. Kimura, and J. Chun. 1998. A single receptor encoded by vzg-1/lpA1/edg-2 couples to G proteins and mediates multiple cellular responses to lysophosphatidic acid. *Proc. Natl. Acad. Sci. USA.* **95:** 6151–6156.
29. Kranenburg, O., M. Poland, M. Gebbink, L. Oomen, and W. H. Moolenaar. 1997. Dissociation of LPA-induced cytoskeletal contraction from stress fiber formation by differential localization of RhoA. *J. Cell Sci.* **110:** 2417–2427.
30. Kranenburg, O., M. Poland, F. P. van Horck, D. Drechsel, A. Hall, and W. H. Moolenaar. 1999. Activation of RhoA by lysophosphatidic acid and Galpha12/13 subunits in neuronal cells: induction of neurite retraction. *Mol. Biol. Cell.* **10:** 1851–1857.
31. Smalheiser, N. R., and J. Y. Ali. 1994. Acute neurite retraction triggered by lysophosphatidic acid: timing of the inhibitory effects of genistein. *Brain Res.* **660:** 309–318.
32. Fukushima, N., D. Furuta, and T. Tsujiuchi. 2011. Coordinated interactions between actin and microtubules through crosslinkers in neurite retraction induced by lysophosphatidic acid. *Neurochem. Int.* **59:** 109–113.
33. Kimura, Y., A. Schmitt, N. Fukushima, I. Ishii, H. Kimura, A. R. Nebreda, and J. Chun. 2001. Two novel Xenopus homologs of mammalian LP(A1)/EDG-2 function as lysophosphatidic acid receptors in Xenopus oocytes and mammalian cells. *J. Biol. Chem.* **276:** 15208–15215.
34. Ishii, I., J. J. Contos, N. Fukushima, and J. Chun. 2000. Functional comparisons of the lysophosphatidic acid receptors, LP(A1)/VZG-1/EDG-2, LP(A2)/EDG-4, and LP(A3)/EDG-7 in neuronal cell lines using a retrovirus expression system. *Mol. Pharmacol.* **58:** 895–902.
35. Contos, J. J. A., N. Fukushima, J. A. Weiner, D. Kaushal, and J. Chun. 2000. Requirement for the lpA1 lysophosphatidic acid receptor gene in normal suckling behavior. *Proc. Natl. Acad. Sci. USA.* **97:** 13384–13389.
36. Fukushima, N., J. A. Weiner, and J. Chun. 2000. Lysophosphatidic acid (LPA) is a novel extracellular regulator of cortical neuroblast morphology. *Dev. Biol.* **228:** 6–18.
37. Hecht, J. H., J. A. Weiner, S. R. Post, and J. Chun. 1996. Ventricular zone gene-1 (vzg-1) encodes a lysophosphatidic acid receptor expressed in neurogenic regions of the developing cerebral cortex. *J. Cell Biol.* **135:** 1071–1083.
38. Kingsbury, M. A., S. K. Rehen, J. J. A. Contos, C. M. Higgins, and J. Chun. 2003. Non-proliferative effects of lysophosphatidic acid enhance cortical growth and folding. *Nat. Neurosci.* **6:** 1292–1299.

39. Dottori, M., J. Leung, A. M. Turnley, and A. Pebay. 2008. Lysophosphatidic acid inhibits neuronal differentiation of neural stem/progenitor cells derived from human embryonic stem cells. *Stem Cells.* **26:** 1146–1154.
40. Shin, S., M. Mitalipova, S. Noggle, D. Tibbitts, A. Venable, R. Rao, and S. L. Stice. 2006. Long-term proliferation of human embryonic stem cell-derived neuroepithelial cells using defined adherent culture conditions. *Stem Cells.* **24:** 125–138.
41. Hurst, J. H., J. Mumaw, D. W. Machacek, C. Sturkie, P. Callihan, S. L. Stice, and S. B. Hooks. 2008. Human neural progenitors express functional lysophospholipid receptors that regulate cell growth and morphology. *BMC Neurosci.* **9:** 118.
42. Yu, J., M. A. Vodyanik, K. Smuga-Otto, J. Antosiewicz-Bourget, J. L. Frane, S. Tian, J. Nie, G. A. Jonsdottir, V. Ruotti, R. Stewart, et al. 2007. Induced pluripotent stem cell lines derived from human somatic cells. *Science.* **318:** 1917–1920.
43. Reubinoff, B. E., M. F. Pera, C. Y. Fong, A. Trounson, and A. Bongso. 2000. Embryonic stem cell lines from human blastocysts: somatic differentiation in vitro. *Nat. Biotechnol.* **18:** 399–404.
44. Liu, J., P. J. Verma, M. V. Evans-Galea, M. B. Delatycki, A. Michalska, J. Leung, D. Crombie, J. P. Sarsero, R. Williamson, M. Dottori, et al. 2011. Generation of induced pluripotent stem cell lines from Friedreich ataxia patients. *Stem Cell Rev.* **7:** 703–713.
45. Reubinoff, B. E., P. Itsykson, T. Turetsky, M. F. Pera, E. Reinhartz, A. Itzik, and T. Ben-Hur. 2001. Neural progenitors from human embryonic stem cells. *Nat. Biotechnol.* **19:** 1134–1140.
46. Song, B., G. Sun, D. Herszfeld, A. Sylvain, N. V. Campanale, C. E. Hirst, S. Caine, H. C. Parkington, M. A. Tonta, H. A. Coleman, et al. 2012. Neural differentiation of patient specific iPS cells as a novel approach to study the pathophysiology of multiple sclerosis. *Stem Cell Res.* **8:** 259–273.
47. Chen, G., Z. Hou, D. R. Gulbranson, and J. A. Thomson. 2010. Actin-myosin contractility is responsible for the reduced viability of dissociated human embryonic stem cells. *Cell Stem Cell.* **7:** 240–248.
48. Ohta, H., K. Sato, N. Murata, A. Damirin, E. Malchinkhuu, J. Kon, T. Kimura, M. Tobo, Y. Yamazaki, T. Watanabe, et al. 2003. Ki16425, a subtype-selective antagonist for EDG-family lysophosphatidic acid receptors. *Mol. Pharmacol.* **64:** 994–1005.
49. Leesnitzer, L. M., D. J. Parks, R. K. Bledsoe, J. E. Cobb, J. L. Collins, T. G. Consler, R. G. Davis, E. A. Hull-Ryde, J. M. Lenhard, L. Patel, et al. 2002. Functional consequences of cysteine modification in the ligand binding sites of peroxisome proliferator activated receptors by GW9662. *Biochemistry.* **41:** 6640–6650.
50. Vogelsgesang, M., A. Pautsch, and K. Aktories. 2007. C3 exoenzymes, novel insights into structure and action of Rho-ADP-ribosylating toxins. *Naunyn Schmiedebergs Arch. Pharmacol.* **374:** 347–360.
51. Ishizaki, T., M. Uehata, I. Tamechika, J. Keel, K. Nonomura, M. Maekawa, and S. Narumiya. 2000. Pharmacological properties of Y-27632, a specific inhibitor of rho-associated kinases. *Mol. Pharmacol.* **57:** 976–983.
52. Luo, L. 2002. Actin cytoskeleton regulation in neuronal morphogenesis and structural plasticity. *Annu. Rev. Cell Dev. Biol.* **18:** 601–635.
53. Bilic, J., and J. C. I. Belmonte. 2012. Concise review: Induced pluripotent stem cells versus embryonic stem cells: close enough or yet too far apart? *Stem Cells.* **30:** 33–41.
54. Pébay, A., R. C. Wong, S. M. Pitson, E. J. Wolvetang, G. S. Peh, A. Filipczyk, K. L. Koh, I. Tellis, L. T. Nguyen, and M. F. Pera. 2005. Essential roles of sphingosine-1-phosphate and platelet-derived growth factor in the maintenance of human embryonic stem cells. *Stem Cells.* **23:** 1541–1548.
55. Bächner, D., M. Ahrens, N. Betat, D. Schröder, and G. Gross. 1999. Developmental expression analysis of murine autotaxin (ATX). *Mech. Dev.* **84:** 121–125.
56. Dorsam, R. T., and J. S. Gutkind. 2007. G-protein-coupled receptors and cancer. *Nat. Rev. Cancer.* **7:** 79–94.
57. Holtsberg, F. W., M. R. Steiner, J. N. Keller, R. J. Mark, M. P. Mattson, and S. M. Steiner. 1998. Lysophosphatidic acid induces necrosis and apoptosis in hippocampal neurons. *J. Neurochem.* **70:** 66–76.
58. Cui, H-L., and J. Qiao. 2007. Effect of lysophosphatidic acid on differentiation of embryonic neural stem cells into neuroglial cells in rats in vitro. *Sheng Li Xue Bao (Acta Physiologica Sinica).* **59:** 759–764.
59. Cui, H.-L., and J.-T. Qiao. 2006. Promotive action of lysophosphatidic acid on proliferation of rat embryonic neural stem cells and their differentiation to cholinergic neurons in vitro. *Sheng Li Xue Bao (Acta Physiologica Sinica).* **58:** 547–555.
60. Spohr, T. C., J. W. Choi, S. E. Gardell, D. R. Herr, S. K. Rehen, F. C. A. Gomes, and J. Chun. 2008. Lysophosphatidic acid receptor-dependent secondary effects via astrocytes promote neuronal differentiation. *J. Biol. Chem.* **283:** 7470–7479.
61. Tigyi, G., D. J. Fischer, A. Sebok, C. Yang, D. L. Dyer, and R. Miledi. 1996. Lysophosphatidic acid-induced neurite retraction in PC12 cells: control by phosphoinositide-Ca2+ signaling and Rho. *J. Neurochem.* **66:** 537–548.
62. Watanabe, K., M. Ueno, D. Kamiya, A. Nishiyama, M. Matsumura, T. Wataya, J. B. Takahashi, S. Nishikawa, K. Muguruma, and Y. Sasai. 2007. A ROCK inhibitor permits survival of dissociated human embryonic stem cells. *Nat. Biotechnol.* **25:** 681–686.
63. Damoiseaux, R., S. P. Sherman, J. A. Alva, C. Peterson, and A. D. Pyle. 2009. Integrated chemical genomics reveals modifiers of survival in human embryonic stem cells. *Stem Cells.* **27:** 533–542.
64. Koyanagi, M., J. Takahashi, Y. Arakawa, D. Doi, H. Fukuda, H. Hayashi, S. Narumiya, and N. Hashimoto. 2008. Inhibition of the Rho/ROCK pathway reduces apoptosis during transplantation of embryonic stem cell-derived neural precursors. *J. Neurosci. Res.* **86:** 270–280.
65. Harb, N., T. K. Archer, and N. Sato. 2008. The Rho-Rock-Myosin signaling axis determines cell-cell integrity of self-renewing pluripotent stem cells. *PLoS ONE.* **3:** e3001.
66. Mills, J. C., N. L. Stone, J. Erhardt, and R. N. Pittman. 1998. Apoptotic membrane blebbing is regulated by myosin light chain phosphorylation. *J. Cell Biol.* **140:** 627–636.
67. Dubreuil, C. I., M. J. Winton, and L. McKerracher. 2003. Rho activation patterns after spinal cord injury and the role of activated Rho in apoptosis in the central nervous system. *J. Cell Biol.* **162:** 233–243.
68. Krawetz, R. J., X. Li, and D. E. Rancourt. 2009. Human embryonic stem cells: caught between a ROCK inhibitor and a hard place. *Bioessays.* **31:** 336–343.
69. Ikeda, H., K. Nagashima, M. Yanase, T. Tomiya, M. Arai, Y. Inoue, K. Tejima, T. Nishikawa, M. Omata, S. Kimura, et al. 2003. Involvement of Rho/Rho kinase pathway in regulation of apoptosis in rat hepatic stellate cells. *Am. J. Physiol. Gastrointest. Liver Physiol.* **285:** G880–G886.
70. Lai J. M., C. Y. Lu, H. F. Yang-Yen, and Z. F. Chang. 2001. Lysophosphatidic acid promotes phorbol-ester-induced apoptosis in TF-1 cells by interfering with adhesion. *Biochem. J.* **359:** 227–233.
71. Picard-Riera, N., B. Nait-Oumesmar, and A. Baron-Van Evercooren. 2004. Endogenous adult neural stem cells: limits and potential to repair the injured central nervous system. *J. Neurosci. Res.* **76:** 223–231.
72. Jin, K., X. Wang, L. Xie, X. O. Mao, and D. A. Greenberg. 2010. Transgenic ablation of doublecortin-expressing cells suppresses adult neurogenesis and worsens stroke outcome in mice. *Proc. Natl. Acad. Sci. USA.* **107:** 7993–7998.
73. Nakayama, D., T. Matsuyama, H. Ishibashi-Ueda, T. Nakagomi, Y. Kasahara, H. Hirose, A. Kikuchi-Taura, D. M. Stern, H. Mori, and A. Taguchi. 2010. Injury-induced neural stem/progenitor cells in post-stroke human cerebral cortex. *Eur. J. Neurosci.* **31:** 90–98.
74. Richardson, R. M., A. Singh, D. Sun, H. L. Fillmore, D. W. Dietrich 3rd, and M. R. Bullock. 2010. Stem cell biology in traumatic brain injury: effects of injury and strategies for repair. *J. Neurosurg.* **112:** 1125–1138.
75. Fukushima, N. 2004. LPA in neural cell development. *J. Cell. Biochem.* **92:** 993–1003.
76. Steiner, M. R., J. R. Urso, J. Klein, and S. M. Steiner. 2002. Multiple astrocyte responses to lysophosphatidic acids. *Biochim. Biophys. Acta.* **1582:** 154–160.
77. Eichholtz, T., K. Jalink, I. Fahrenfort, and W. H. Moolenaar. 1993. The bioactive phospholipid lysophosphatidic acid is released from activated platelets. *Biochem. J.* **291:** 677–680.
78. Tigyi, G., L. Hong, M. Yakubu, H. Parfenova, M. Shibata, and C. W. Leffler. 1995. Lysophosphatidic acid alters cerebrovascular reactivity in piglets. *Am. J. Physiol.* **268:** H2048–H2055.
79. Savaskan, N. E., L. Rocha, M. R. Kotter, A. Baer, G. Lubec, L. A. van Meeteren, Y. Kishi, J. Aoki, W. H. Moolenaar, R. Nitsch, et al. 2007. Autotaxin (NPP-2) in the brain: cell type-specific expression and regulation during development and after neurotrauma. *Cell. Mol. Life Sci.* **64:** 230–243.
80. Goldshmit, Y., R. Matteo, T. Sztal, F. Ellett, F. Frisca, K. Moreno, D. Crombie, G. J. Lieschke, P. D. Currie, R. A. Sabbadini, et al. 2012. Blockage of lysophosphatidic acid signaling improves spinal cord injury outcomes. *Am. J. Pathol.* **181:** 978–992.
81. Kimura, A., T. Ohmori, Y. Kashiwakura, R. Ohkawa, S. Madoiwa, J. Mimuro, K. Shimazaki, Y. Hoshino, Y. Yatomi, and Y. Sakata. 2008. Antagonism of sphingosine 1-phosphate receptor-2 enhances migration of neural progenitor cells toward an area of brain. *Stroke.* **39:** 3411–3417.